ARTICLE IN PRESS

ELSEVIER

Journal of Nuclear Materials 307–311 (2002) 159–170

journal of nuclear materials

www.elsevier.com/locate/jnucmat

Section 3. Mechanical and microstructure effects in irradiated metals

Experiment-based modelling of hardening and localized plasticity in metals irradiated under cascade damage conditions

B.N. Singh [a,*], N.M. Ghoniem [b], H. Trinkaus [c]

[a] *Materials Research Department, Risø National Laboratory, DK-4000 Roskilde, Denmark*
[b] *Mechanical and Aerospace Engineering Department, UCLA, Los Angeles, CA 90095-1597, USA*
[c] *Institut für Festkörperforschung, Forschungszentrum Jülich, D-52425 Jülich, Germany*

Abstract

The analysis of the available experimental observations shows that the occurrence of a sudden yield drop and the associated plastic flow localization are the major concerns regarding the performance and lifetime of materials exposed to fission or fusion neutrons. In the light of the known mechanical properties and microstructures of the as-irradiated and irradiated and deformed materials, it has been argued that the increase in the upper yield stress, the sudden yield drop and the initiation of plastic flow localization, can be rationalized in terms of the cascade induced source hardening (CISH) model. Various aspects of the model (main assumptions and predictions) have been investigated using analytical calculations, 3-D dislocation dynamics and molecular dynamics simulations. The main results and conclusions are briefly summarized. Finally, it is pointed out that even though the formation of cleared channels may be rationalized in terms of climb-controlled glide of the source dislocation, a number of problems regarding the initiation and the evolution of these channels remain unsolved.

1. Introduction

It is well established that neutron irradiation at temperatures below the recovery stage V causes a large increase in the yield strength but at the same time leads to a severe reduction in the ductility (commonly known as low temperature embrittlement). This phenomenon is, in fact, a very good example of the so-called 'Wigner disease' [1] caused by energetic neutrons and has been a matter of serious concern for the nuclear technology from the point of view of lifetime of structural components exposed to fission or fusion neutrons. Since the early investigations of radiation hardening already in the 1950s and 1960s [2–5], a large amount of both experimental and theoretical results have become available on this topic (see Ref. [6] for a critical review).

In spite of more than 40 years of extensive investigations, unfortunately our understanding of this phenomenon still remains rather nebulous and the old concern regarding the low temperature embrittlement still lingers on. A close look at the literature suggests several reasons for this predicament. First of all, until recently, there has been a lack of detailed information regarding the complex nature of the damage production and accumulation during neutron irradiation. Secondly, the traditional assumptions that the accumulation of defect clusters during neutron irradiation occurs in a homogeneous fashion and that during post-irradiation deformation dislocations are generated homogeneously are not consistent with experimental observations showing, for example, segregation in the form of dislocation decoration and rafts of loops and generation of dislocation during deformation at the sites of stress/strain

* Corresponding author. Tel.: +45-4677 5709; fax: +45-4677 5758.
E-mail address: bachu.singh@risoe.dk (B.N. Singh).

0022-3115/02/$ - see front matter
PII: S0022-3115(02)01095-4

concentration (see later for details). Thirdly, the occurrence of an abrupt yield drop and its implications to the initiation and continuation of plastic deformation in materials irradiated and tested at temperatures below the recovery stage V has been completely ignored. Finally, even though the loss of ductility caused by neutron irradiation is the most important problem and is the main source of concern regarding materials performance, yet practically no theoretical considerations have been given to this problem until recently.

It is encouraging to note, however, that in recent years some serious efforts have been made to overcome the difficulties outlined above. These efforts have led to some significant progress and have contributed to a better understanding of the effect of irradiation on mechanical performance of irradiated materials. New experimental investigations [7–9], theoretical considerations [6,10] and computer simulations using both molecular dynamics (MD) [11–17] and 3-D dislocation dynamics (DD) [18–21] techniques have provided a great help in identifying the relevant physical processes involved in controlling the increase in the yield strength and the occurrence of a sudden yield drop as well as plastic flow localization. In the present paper an attempt is made to describe first of all a brief synthesis of the current perception of the problem of radiation hardening in terms of the microstructural features induced during irradiation, the impact of these features on the mechanical response and important elements of the microstructure generated during post-irradiation deformation. It will be emphasized that the irradiation induced increase in the yield strength (hardening) and the ensuing plasticity of the irradiated materials should be treated in a consistent manner and should include the appropriate considerations of the main features of the damage production and accumulation under cascade damage conditions.

2. Hardening, flow localization and loss of ductility

Prior to addressing the real issues of hardening and loss of ductility in irradiated materials, let us first consider the general problem of the initiation and continuation of plastic deformation. It is imperative, however, to distinguish between the initiation (yielding) and continuation (work hardening or softening) stages of the plastic flow. It is pertinent to note here that this distinction is of particular importance while considering radiation hardening since most of polycrystalline metals and alloys exhibit an increase in the yield strength but a decrease in the work hardening.

It is well known that the initiation of plastic flow (i.e. yielding) occurs when a significant number of grown-in dislocations are made free (i.e. unlocked) to move and act as dislocation sources. According to Cottrell [22], the slip during deformation is nucleated heterogeneously and the grown-in dislocations (present prior to the application of load) provide the nucleation sites for the slip. The clean grown-in dislocations (i.e. free from impurities) may be able to generate a large number of new dislocations by acting as Frank–Read (F–R) sources [23]. These dislocations will start operating as F–R sources only when the applied stress is sufficient to overcome the restoring force on the dislocations due to their line tension, i.e. when the applied stress is about Gb/l where G is the shear modulus, b the Burgers vector and l the length of dislocation segment (i.e. F–R source) between the pinning points. The multiplication and movement of these free dislocations and the resulting dislocation-dislocation interactions lead to work hardening as deformation continues. As discussed in Ref. [6], this relationship can be used to rationalize the observed yield strength in single crystal and cold-worked polycrystalline copper in the unirradiated condition. Thus, it is the creation of new mobile dislocations by the applied stress which determines the initiation of the plastic flow. In a large and soft single crystal the plastic deformation is known to be initiated at a strain level of as low as 10^{-5} [24].

Clearly, a sufficiently large number of dislocations would have to be generated so that the accumulated plastic strain in a bulk tensile specimen would be large enough to make the yielding of the specimen (i.e. change in elastic to plastic mode of deformation) visible on the stress–strain curve. Normally, in annealed and pure fcc metals, this transition occurs rather smoothly (see Fig. 1). As deformation continues, the interactions between mobile dislocations generated from the F–R sources lead to work hardening. The stress–strain curves shown in Fig. 1 for annealed and cold-worked copper tested at room temperature illustrate this kind of behaviour. Fig. 1 also shows a stress–strain curve for copper containing a fine dispersion of alumina particles ($\sim 2 \times 10^{22}$ m^{-3}) which was also tested in the cold-worked state [25]. It can be readily seen in Fig. 1 that both cold work and dispersion of oxide particles cause a large increase in the yield strength and a correspondingly large decrease in the uniform elongation. However, it is interesting to note that in both cases the work hardening is still positive, indicating that dislocation generation and interactions (i.e. plastic deformation) occur in a relatively homogeneous fashion. Resistance to dislocation motion in the cold-worked material is provided by the forest dislocations [26] and by the oxide particles as well as dislocations in the dispersion hardened copper alloy [27].

Let us now consider the case of irradiation hardening and its impact on the materials performance. As can be seen in Fig. 1, the annealed copper irradiated with fission neutrons at $\sim$50 °C to a displacement dose level of 0.2 dpa and tested at room temperature exhibits a fundamentally different deformation behaviour compared

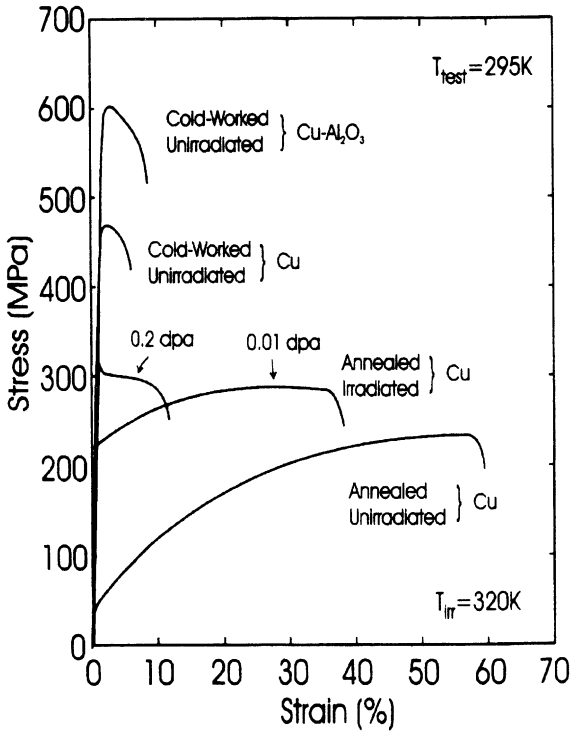

Fig. 1. Stress–strain curves for unirradiated and irradiated copper. For comparison, curves for cold-worked copper and $Cu–Al_2O_3$ alloy are also shown [28].

to the behaviour observed in the unirradiated copper. The occurrence of a sudden yield drop, the loss of work hardening capability and almost a complete lack of uniform elongation are the most significant effects of irradiation on materials performance and lifetime and, therefore, have been considered to be the critical issues from the point of view of practical applications of such materials in neutron environment. Unfortunately, this is not an isolated response of pure copper but is common to most fcc, bcc and hcp metals and alloys [6] irradiated at temperatures below the recovery stage V (i.e. <0.3–$0.4\ T_m$ where T_m is the melting temperature). The behaviour described above demonstrates that irradiated materials (to doses beyond a certain dose level) are unable to deform plastically in a homogeneous manner and that the materials response is seriously affected by the localized plastic flow.

Thus, our task is not only to explain the irradiation-induced hardening as such but to construct a model which can, in a consistent manner, rationalize the hardening as well as the sudden yield drop and the resulting flow localization and plastic instability. For such a model to be realistic, it has to be based on experimental observations illustrating (a) the relationship between the as-irradiated microstructure and the mechanical response and (b) changes in the microstructure as a result of deformation. Furthermore, the processes involved in the evolution of the pre-deformation microstructure during irradiation as well as the consequences of interactions between the pre-deformation (as-irradiated) microstructure (e.g. clusters, loops, SFTs and voids) and the deformation-induced dislocations need to be investigated. In recent years, both analytical calculations and computer simulations have been carried out to study these problems. The framework and the main outcome of these studies are synthesized in the following sections. It is appropriate, however, at least in our view, to provide a brief description of the important features of the pre-deformation microstructures (Section 3.1), the significant aspects of the mechanical response of these microstructures to applied stress (Section 3.2) during deformation and the changes in the initial microstructure due to the applied stress (Section 3.3) prior to describing the results of theoretical considerations and computer simulations (Section 4).

3. Phenomenology of microstructure and mechanical response

3.1. Irradiation-induced microstructure

The spatial and temporal evolution of defect microstructure under cascade damage conditions is a complex issue and is primarily controlled by the nature of intracascade clustering and properties of clusters of SIAs and vacancies. The consequences of intracascade events, features of the primary damage production and aspects of temporal and spatial evolution of defect microstructure have been reviewed in recent publications [e.g. 11,14,28,29] and will not be repeated here. However, in order to understand the observed microstructure, it would be very useful to recognize the following unique and intrinsic features of the primary damage produced in displacement cascades:

(i) A substantial fraction of primary damage is produced in the form of clusters of SIAs and vacancies. Both glissile and sessile SIA clusters are produced.
(ii) Glissile clusters/loops are highly mobile in the direction of their Burgers vector and may change their Burgers vector while diffusing one-dimensionally due to interactions with other loops (glissile or sessile) and thermal activation.
(iii) The crystal structure has significant effects on clustering efficiency as well as properties of SIA clusters. At a given recoil energy and temperature, the clustering efficiency of SIAs, for example, is considerably higher in fcc copper than that in bcc iron whereas practically all SIA clusters produced in cascades in bcc iron are glissile, only a relatively small fraction is found to be glissile in fcc copper.

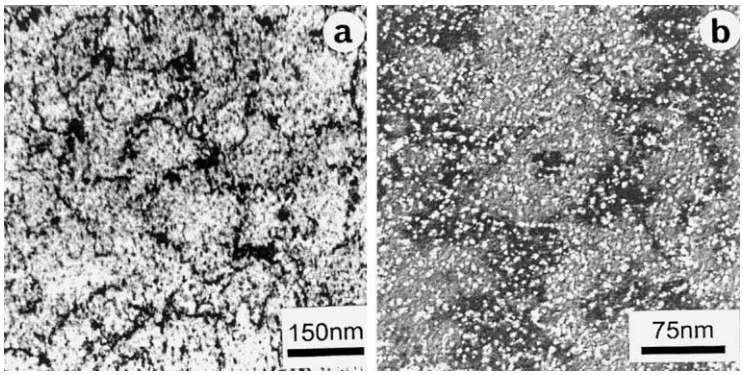

Fig. 2. Loop and SFT microstructures of copper irradiated at 100 °C to 0.3 dpa: (a) loops and raft-like agglomerates of loops, (b) SFTs with a relatively homogeneous spatial distribution [8].

(iv) SIA clusters interact and segregate both within a cascade and between the cascades.

The microstructure of even simple materials (e.g. pure metals and alloys) irradiated with fission or fusion neutrons at relatively low temperature ($<0.4\ T_m$) is composed of submicroscopic and microscopic defect clusters and dislocation segments. It is important to note that, in addition, both the residual and transmutational impurity atoms produced during irradiation may segregate on grain boundaries, grown-in dislocations, defect clusters and loops formed during irradiation and may even form submicroscopic or microscopic precipitates. Furthermore, it is rather common that the SIA clusters accumulate in a spatially segregated form whereas the vacancy clusters evolve with a homogeneous distribution. This is illustrated in Fig. 2 for neutron irradiated copper at 100 °C to a displacement dose level of 0.3 dpa [8]. Fig. 2(a) shows the segregation of SIA loops in raft-like agglomerates with a relatively low density. The same specimens also contain a high density of SFTs (4.3×10^{23} m^{-3}) with a fairly homogeneous distribution (Fig. 2(b)).

The evolution of microstructure in bcc iron and molybdenum is qualitatively different from that observed in fcc copper. In Fe and Mo no SFTs are observed. Instead, a high density of nanovoids are formed in Fe [30,31], Mo [32] and TZM [33]. In addition, in Fe, Mo and TZM, the loop microstructure is dominated by 'rafts' of loops (e.g. [31,33,34]). The dose dependence of raft formation in single crystal Mo [34] and the temperature dependence of raft formation in TZM [33] have also been reported. An example of raft formation in TZM [33] irradiated at 350 °C ($\sim 0.22\ T_m$) is shown in Fig. 3. In both cases, the rafts of loops co-exist with a high density of voids [31,33]. Very recently rafts of loops and voids have been found to co-exist also in bcc iron irradiated at $\sim 0.19\ T_m$ [31]. It is also of interest to note that the density of SIA clusters/loops in iron, Mo and TZM at a given dose level and below the recovery stage V is considerably lower (about two orders of magnitude) than the density of vacancy clusters (SFTs) in fcc copper (see [33–36] for comparison).

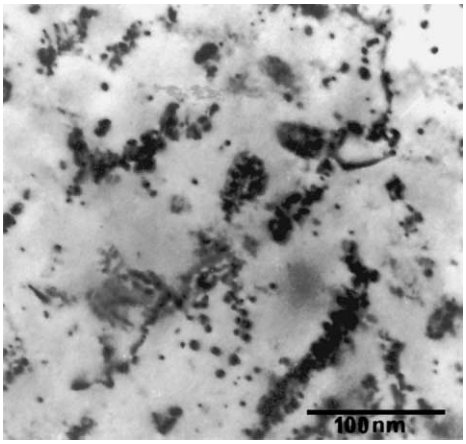

Fig. 3. TEM micrographs showing rafts of loops formed in TZM (a molybdenum alloy containing 0.5% Ti and 0.1% Zr) during neutron irradiation at 350 °C to a dose level of 0.16 dpa [33].

Finally, it should be mentioned that during neutron irradiation at low temperatures (<0.3–$0.4\ T_m$) the grown-in dislocations have been observed to be decorated with an 'atmosphere' of SIA loops. The topic has been reviewed in [10]. It should be noted that the decorated dislocations are observed in single crystal Mo [10] at a much lower dose level (5×10^{-4} dpa) than the dose level at which the rafts of loops get established [34]. Although there is no direct evidence illustrating the segregation of the residual impurities or/and transmutational impuri-ties on grown-in dislocations or on the individual SIA loops in the atmosphere of loops decorating the grown-in dislocations, the possibility of

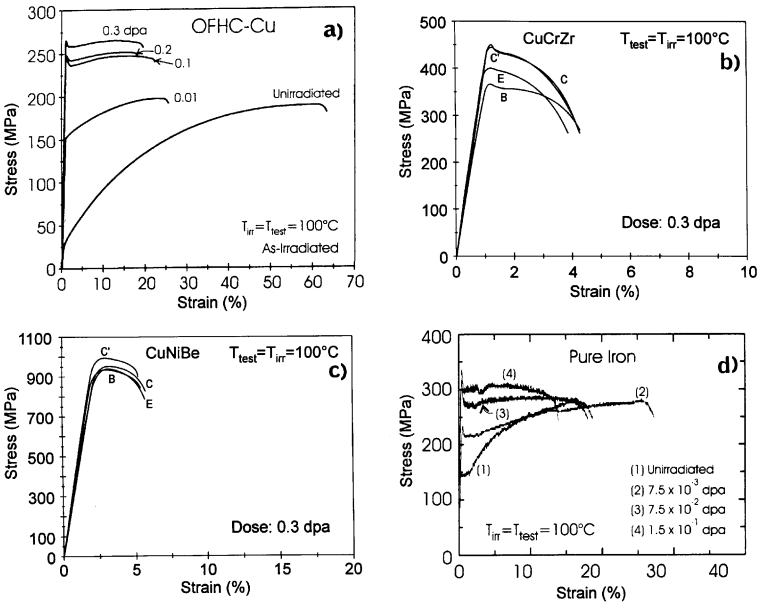

Fig. 4. Stress–strain curves illustrating the effect of irradiation on mechanical response of (a) Cu [8], (b) CuCrZr alloy, (c) CuNiBe alloy [38,39] and (d) Fe [37] irradiated with fission neutrons at 100 °C to different dose levels. E, B, C and C′ in (b) and (c) refer to different heat treatments: E (ageing (475 °C/30 min) + water quench (WQ)); B (E + ann. (950 °C/30 min) + furnace cooling (FC) + re-ageing (475 °C/30 min) + FC); C (B + ann. (350 °C/100 h) + FC); C′ (E + ann. (350 °C/100 h) + FC).

irradiation-induced segregation and its effects cannot be ruled out.

In summary, it should be emphasized that while considering the hardening effects of irradiation-induced defects and their clusters, the effect of both homogeneously and inhomogeneously distributed clusters should be taken into account. Particular attention should be paid to the presence of the decorated dislocations and 'rafts' of loops. Distinction should be also made between SFTs and nanovoids since the strength of interactions between SFTs and voids and moving dislocations on the glide planes are likely to be different.

3.2. Mechanical response

In the following we shall consider the response of irradiated materials under the condition of uniaxial tensile loading. It is well established that neutron irradiation at temperatures below stage V causes the following major changes in materials response:

(i) a substantial increase in the yield stress,
(ii) a sudden yield drop beyond a certain dose level,
(iii) a significant decrease in work hardening causing in some cases even plastic instability (necking and triaxiality),
(iv) a drastic decrease in uniform elongation leading in some cases to brittle fracture.

Some examples of stress–strain curves illustrating the effect of irradiation on mechanical response are shown in Fig. 4 for (a) pure copper [8], (b) CuCrZr alloy [38,39], (c) CuNiBe alloy [38,39] and (d) pure iron [37] irradiated at 100 °C with fission neutrons. Pure copper and iron specimens were irradiated in annealed condition whereas CuCrZr and CuNiBe specimens were given different heat treatments [38,39] after prime ageing and then irradiated. Pure iron specimens were irradiated to displacement doses of 7.5×10^{-3}, 7.5×10^{-2} and 1.5×10^{-1} dpa. CuCrZr and CuNiBe alloys are precipitation hardened alloys with precipitate densities of 3×20^{22} m^{-3} and 5×10^{23} m^{-3}, respectively. The precipitate sizes were in the range of 4.5–5.6 nm in the CuCrZr (B, E) alloy and 3.8–6.6 nm in the CuNiBe (B, E) alloy. In addition, CuCrZr specimens contained $\sim 5.6 \times 10^{23}$ m^{-3} SFTs with an average size of 2.3 nm [38,39]. Because of the high density of precipitates with strong strain field contrast, no SFTs could be identified in the CuNiBe alloy.

As can be seen in Fig. 4, although irradiated copper and iron specimens exhibit yield drop, the deformation behaviour beyond the yield drop is somewhat different in the two cases. Clearly, the irradiation has the most dramatic effect on the mechanical performance of the CuCrZr alloy. In contrast, no yield drop is observed in the irradiated CuNiBe alloy even though there is a very substantial increase in the yield stress and a drastic decrease in the uniform elongation due to irradiation. It

should be added here that metals and alloys dispersion strengthened with strong oxide particles do not exhibit yield drop after neutron irradiation either [38–40].

3.3. Post-deformation microstructure in irradiated materials

First of all, it should be noted that only a limited amount of information is available on the post-deformation microstructure of irradiated materials. However, the available results of TEM investigations clearly demonstrate that the deformation-induced microstructure at least in pure metals irradiated to low doses (<0.1 dpa) is qualitatively different from the microstructure observed in specimens irradiated to higher doses (>0.1 dpa) and then deformed [8,35,40].

In low dose specimens, deformation is found to generate dislocations throughout the whole specimen. The motion and interactions of these freshly generated dislocations among themselves and with the irradiation-induced defect clusters lead to a relatively homogeneously distributed high density of dislocation segments and rather loose dislocation walls (Fig. 5(a)). The presence of irradiation-induced defect clusters (acting as obstacles to dislocation motion) seem to prevent the formation of strong cell structure with thick dislocation walls, as is commonly observed in the unirradiated and deformed materials. As can be seen in Fig. 5(b), the deformation of irradiated and annealed (at 300 °C for 50 h) specimen does indeed lead to a strong cell structure (similar to that in unirradiated copper) since a large fraction of the irradiation-induced defect clusters anneal out during annealing at 300 °C [8]. Note, that these low dose specimens do not exhibit yield drop.

The post-deformation microstructure in specimens irradiated to higher doses (>0.1 dpa) is qualitatively different from that in the low dose (<0.1 dpa) specimens. First, at the higher dose (>0.1 dpa) levels, the plastic deformation occurs in a localized fashion and seems to be concentrated mainly in the 'cleared channels'. Fig. 6 shows some examples of cleared channel formation in (a) single crystal Mo, (b,c) polycrystal copper and (d) CuCrZr alloy. Secondly, practically no fresh dislocations are generated during deformation in the volumes between the cleared channels. It should be mentioned that in some cases (e.g. copper irradiated at 100 °C, Fig. 6(b) and (c), [8]) a few dislocations have been found to be generated in the volumes between the cleared channels. In most cases, the cleared channels have been found to be almost completely free of irradiation-induced defect clusters.

The formation of cleared channels has been observed in a number of metals and alloys irradiated and deformed at temperatures below the recovery stage V. Results suggest that the width of the channels is rather insensitive to material variables (composition, crystal structure and melting temperature) as well as the irradiation variables (damage rate and displacement dose level). It is very interesting to note that the cleared channels are formed in copper at a deformation temperature of as low as 4 K [41]. Furthermore, the channel width increases only by a factor of about two by increasing the test temperature from 4 to 295 K. An important implication of these results is that the process controlling the channel formation and the width of the channels may be athermal.

It is relevant to note that the cleared channels are formed even in the CuCrZr alloy (Fig. 6(d)) [42] containing 3×10^{22} m^{-3} precipitates and 5.6×10^{23} m^{-3} SFTs [38]. Furthermore, the formation of the cleared channels in this material is generally associated with relatively large inclusions of Zr. The CuNiBe and Cu–Al_2O_3 alloys, on the other hand, neither exhibit the yield drop nor show the evidence for the formation of cleared channels.

Finally, it should be recognized that at present there exists no clear experimental evidence as to when (i.e. at what strain/stress level) and where in the irradiated

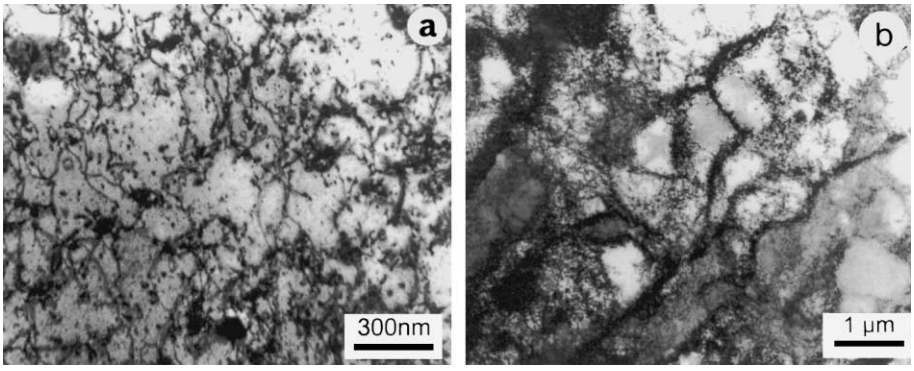

Fig. 5. Post-deformation microstructure of low dose (0.01 dpa) neutron irradiated copper at 100 °C: (a) tensile tested in the as-irradiated condition and (b) tested after post-irradiation annealing at 300 °C for 50 h [8].

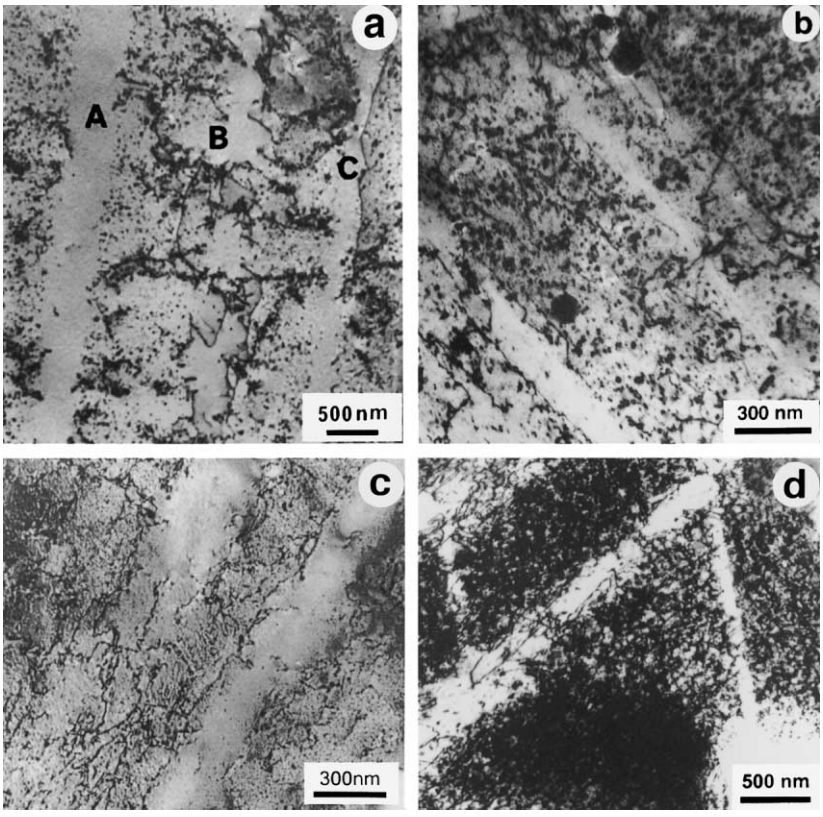

Fig. 6. Some examples of cleared channel formation in neutron irradiated metals: (a) single crystal Mo [34] (50 °C, 5.4×10^{-4} dpa), (b) copper [8] (100 °C, 10^{-2} dpa), (c) copper [8] (100 °C, 0.3 dpa), (d) CuCrZr alloy [42] (50 °C, 0.3 dpa). In Fig. 6(a), A–C refer to three different cleared channels.

material the cleared channels are initiated. TEM results on irradiated and deformed copper and CuCrZr alloy obtained very recently suggest, however, that some specific sites (e.g. ledges) at twin boundaries and grain boundaries may act as the initiation sites for the cleared channel formation [9].

4. Theoretical treatments and computer modelling

The main features of the damage accumulation, its impact on the deformation behaviour and of the post-deformation microstructure described in the previous sections points to the following issues that must be addressed in order to establish a physically consistent understanding of the radiation hardening, flow localization and loss of ductility:

(a) Dislocation decoration and raft formation.
(b) A large increase in the yield stress, followed by a sudden yield drop.
(c) Formation of cleared channels and plastic flow localization.
(d) Activities and mechanisms of defect sweeping in the cleared channels.
(e) Mechanical response of a material containing 'soft' cleared channels and 'hard' matrix (i.e. volumes between the cleared channels).

4.1. Analytical calculations

In the past, the increase in the yield strength due to irradiation has been attributed to defect clusters, loops and SFTs which may act as 'Orowan-type' obstacles [27] to dislocation motion [43]. This is commonly known as dispersed barrier hardening (DBH) model. In recent years, it has been argued, however, that the DBH model is not adequate to explain the occurrence of a sudden yield drop and the localization of plastic flow immediately beyond the yield stress [6,10]. In view of the experimental observations summarized in Section 3, the whole problem was reanalysed. The reanalysis led to a new model called the cascade-induced source hardening (CISH) model [6,10].

The main thesis of the CISH model is that during irradiation under cascade damage conditions most of

the F–R sources (i.e. grown-in dislocations) get decorated by an 'atmosphere' of small SIA clusters or loops (Section 3). As a result, the generation of dislocations necessary for the initiation of plastic deformation is prevented until a stress level is reached at which the decorated dislocations can be 'unlocked' from their atmosphere. The unlocking stress should then correspond to the upper yield stress. It has been further argued that if the dislocation decoration is very dense, requiring a very high stress level to unlock the dislocations, the generation of dislocations may occur at the sites of stress/strain concentrations in the material (e.g. surfaces, grain boundaries, inclusions etc.) with a high stress concentration factor [28]. Furthermore, it is possible that grown-in dislocations do not get equally heavily decorated during irradiation (since, for instance, their character (edge/screw) is different), and hence the lightly decorated dislocations may get activated as dislocation sources particularly in the vicinity of the sites of stress/strain singularities. Thus, a sudden generation and release of a large number of dislocations would explain the observation of a sudden yield drop [44]. It should be mentioned here that the effect of irradiation-induced segregation of impurity atoms on the grown-in dislocations and the loops decorating them could be treated within the framework of the CISH model.

According to the CISH model, the resolved shear stress, τ, necessary to unlock a decorated dislocation is given by (6,10)

$$\tau \cong 0.1G(b/L)(d/y)^2 \quad (1)$$

where L is the distance between the loops of diameter d in the decoration and y is the 'stand-off' distance between the edge dislocation and the loop ensemble in the decoration along the length of the decorated dislocation. In order to justify the applicability of Eq. (1), we need to validate the concept of stand-off distance as well as of the phenomenon of dislocation decoration. Note that the loops (in the decoration) have the same Burgers vector as the edge dislocation. A lower bound value of y has been estimated to be of the order of the radius of loops in the decoration [6]. The operating mechanism here is considered to be the change in the Burgers vector of the loops due to the stress field of the edge dislocation. At elevated temperatures, conservative climb of the SIA loops may play a decisive role in determining the effective 'stand-off' distance. In Ref. [6], the break-up of small SIA clusters into single interstitial atoms under the combined influence of a large hydrostatic tension from the edge dislocation and the ambient temperature has been considered to be an alternative mechanism for the occurrence of stand-off distance.

Detailed analytical calculations have been carried out to examine the formation of dislocation decoration under the condition of production of glissile SIA clusters

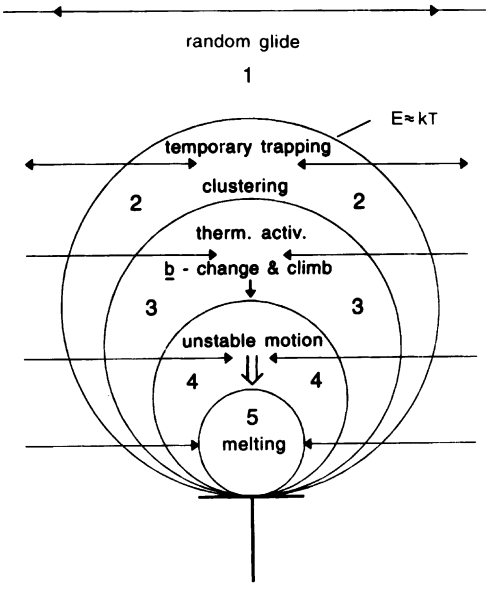

Fig. 7. Schematic illustration of characteristic regions (no absolute and relative size scales) in the interaction of a glissile interstitial loop with an edge dislocation [10].

[10]. Fig. 7 shows different regions of interaction between a glissile SIA loop and an edge dislocation. The gliding SIA clusters/loops in regions 2 and 3 are likely to be trapped permanently and will accumulate and grow whereas those entering region 4 are likely to get absorbed in the dislocation core. Thermally activated Burgers vector change and conservative climb of the loops are considered to be the main processes determining their absorption into the edge dislocation.

4.2. Dislocation dynamics calculations

It should be noted that the result shown in Eq. (1) is obtained using isotropic elasticity theory, rigid-dislocation and infinitesimal loop approximation. However, since the calculation involves very close distance interactions between the loops and the grown-in dislocations as well as inter-cluster interactions, it is possible that the scaling of the unlocking stress with the 'stand-off' distance given by Eq. (1) may not be completely accurate. In order to test this, numerical calculations using 3-D DD were initiated to investigate the question of 'stand-off' distance and dislocation decoration [45,46]. These calculations validated the concept of 'stand-off' distance and demonstrated that the clusters closer to the dislocation than the 'stand-off' distance will be absorbed by unfaulting and or changing the Burgers vector of small Frank loops under a high torque.

The 3-D DD methodology has been used also to calculate the unlocking stress for a dislocation from its decoration containing an atmosphere of loops [20]. The

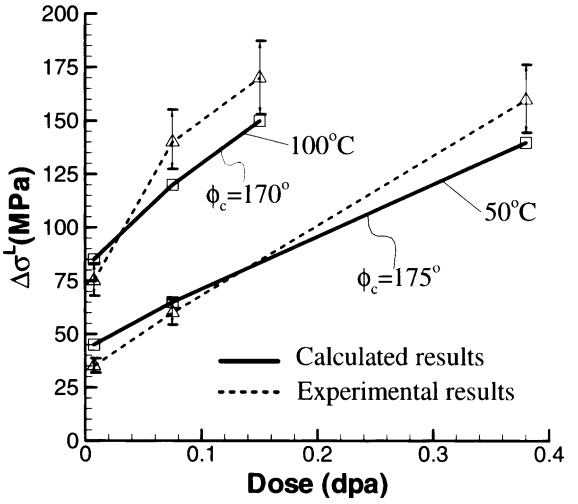

Fig. 8. Dose dependence of calculated and experimentally measured values of increase in the lower yield strength due to irradiation in pure iron neutron irradiated at 50 and 100 °C.

results have been found to be consistent with the experimental values of the upper yield stress for copper irradiated at ~50 °C to doses higher than 0.01 dpa (Fig. 1) [20]. The results of these calculations are in general agreement with the results of the analytical calculations [6,10]. However, the scaling of the unlocking stress of dislocations from their atmosphere with the 'stand-off' distance, y, as well as with the inter-cluster distance, L, calculated using DD is slightly different from that of the results of analytical calculations (see Figs. 7 and 8 in [20]). This is primarily because the dislocation segments are flexible rather than rigid lines [20] when they move close to the clusters. In the analytical calculation, on the other hand, dislocations are assumed to be rigid.

Recently, the phenomenon of dislocation decoration has been simulated using 3-D DD and kinetic Monte Carlo in bcc iron [21] for an irradiation temperature of 300 K. Simulations have been carried out under the condition where glissile loops interact with each other as well as with a pre-allocated dislocation in the simulation cell. A well-defined decoration is found to occur already in 6 ns (Fig. 2 in [21]), confirming the results of analytical calculations reported in [10].

Thus, the results of the 3-D DD calculations are in agreement with results of analytical calculations reported in [6,10] for the unlocking stress representing the upper yield stress. The question as to how the stress level at the lower yield point is maintained was not addressed by the analytical calculations. It has been shown, on the other hand, that the problem can be treated within the framework of 3-D DD. For this purpose, a detailed computational methodology has been developed to calculate the stress necessary to propagate the dislocations (generated from various sources) on the glide planes containing obstacles (e.g. loops, SFTs, voids) (see [20,21]. For copper neutron irradiated at 50 and 100 °C, the calculated hardening (increase in the yield-stress) at various dose levels agree very well with the experimental results [20,21]. These calculations were carried out taking SFTs as the main obstacles in the glide planes.

It has been shown recently, however, that the main obstacles to dislocation motion in Fe irradiated at 70 and 100 °C are likely to be nanovoids [30,31]. In the following, we present the results of the 3-D DD calculations of radiation hardening due to dislocation-void interactions and their comparison with experimental results [35,37]. The computational methodology employed in these calculations are the same as described in [20,21]. Here we assume that under the action of an applied stress dislocations released from sources impinge upon nanovoids and destroy them if the work done by local forces exerted by dislocations on nanovoids exceed a critical value determined by the elastic interaction energy. In the present simulations it is assumed that the nanovoids are destroyed by gliding dislocations once the angle between the arms of the dislocation that surround the voids exceeds a critical value Φ_c. Both experimental and calculated results are quoted in Tables 1 and 2 and are plotted in Fig. 8 as a function of irradiation dose. The calculated and experimental results agree reasonably well. It should be emphasized here that this agreement should be taken with a caution since the results are very sensitive to Φ_c (see Tables 1 and 2) and Φ_c has been used as an adjustable parameter. Clearly, MD simulations are necessary to determine the interaction energy between voids and dislocations.

It is relevant to note here that since the present calculations do not include the contribution of the SIA loops, the calculated $\Delta\sigma^l$ would be an underestimate particularly at higher doses where the loop density and size become significant. At the irradiation temperature of 50 °C, for example, a loop density of $\sim 4 \times 10^{22}$ m^{-3} of ~5 nm in diameter has been reported for a dose level of ~0.38 dpa [35]. This may be the reason why the experimental value of $\Delta\sigma^l$ at the dose level of ~0.38 dpa is noticeably higher than the calculated value (Fig. 8). The same explanation may be valid also for the results for 100 °C (Fig. 8).

As regards the question as to how and where the plastic flow localization is initiated, so far it has not been possible to provide either analytically or numerically a precise and definitive answer. Nonetheless, attempts have been made to identify the mechanisms of flow localization in the form of cleared channels using 3-D dislocation dynamics [20,21]. In these studies, a F–R source is assumed to become operative at a certain stress level. The source dislocation interacts with SFTs (in the case of copper) or voids (in the case of iron) on the glide plane, absorbs the vacancies contained in the SFTs or voids and climbs out of its glide plane by the formation

Table 1
Experimental and calculated values of the increase in the lower yield stress, Δ_{exp}^{l} [35] and $\Delta\sigma_{cal}^{l}$, respectively for pure Fe irradiated at 50 °C to different dose levels

Dose (dpa)	σ_y^u (MPa)	$\Delta\sigma_{Exp}^{u}$ (MPa)	σ_y^l (Mpa)	$\Delta\sigma_{Exp}^{l}$ (MPa)	C_{m_v} (10^{24} M^{-3})	d_v (nm)	$\Delta\sigma_{Cal}^{l}$ (MPa)		
							Critical angles		
							172°	175°	178°
0	235	–	220	–	–	–	–	–	–
0.0075	275	40	245	35	2.5	0.50	65	45	35
0.075	302	67	280	60	4.0	0.51	80	65	45
0.38	414	179	380	160	4.5	1.0	150	140	125

The density, C_{m-u} and size, d_v, of voids are obtained from positron annihilation experiments [30].

Table 2
The same as in Table 1 but for irradiations at 100 °C

Dose (dpa)	σ_y^u (MPa)	$\Delta\sigma_{Exp}^{u}$ (MPa)	σ_y^l (Mpa)	$\Delta\sigma_{Exp}^{l}$ (MPa)	C_{m_v} (10^{24} M^{-3})	d_v (nm)	$\Delta\sigma_{Cal}^{l}$ (MPa)		
							Critical angles		
							165°	170°	175°
0	155	–	140	–	–	–	–	–	–
0.0075	235	80	215	75	2.5	0.51	120	85	45
0.075	320	165	280	140	4.0	0.54	165	120	70
0.15	336	171	310	170	4.0	0.72	180	150	110

$\Delta\sigma_{exp}^{l}$ values are taken from results quoted in [37].

of atomic jogs. This is followed by the subsequent glide motion of the joged dislocation segments on a neighbouring glide plane. This climb-controlled glide mechanism has been shown to create cleared channels in copper [20] and iron [21]. Details of the dislocation – SFTs (and voids) interaction and vacancy absorption in the dislocation core have been studied using MD (see Section 4.3) simulations.

4.3. Molecular dynamics simulations

As indicated already in Section 3, the production of the primary damage under cascade damage conditions in the form of clusters of SIAs and vacancies and the properties of these clusters have been established by MD simulations (see Ref. [14] for details). Naturally, this information must be incorporated in the modelling of the damage accumulation and its impact on mechanical properties (Sections 4.1 and 4.2). It is, for example, the production of glissile SIA clusters that gives rise to dislocation decoration and raft formation which in turn can be used to rationalize the phenomena of hardening, yield drop and plastic flow localization. It is also interesting to note that the fact that practically all SIA clusters produced in Fe are glissile [12] and that vacancy clusters do not collapse into SFTs may be responsible for the formation of a high density of voids in Fe [30,31]. In contrast, a high density of SFTs are produced in copper (e.g. [8,38]). In other words, for a given irradiation condition, the lower yield stress in Fe has to be treated in terms of voids and in Cu in terms of SFTs since these are the dominant obstacles to dislocation motion in pure Fe and Cu, respectively.

In order to test the validity of the application of the linear elasticity theory in the calculation of unlocking stress or dislocation decoration (see Sections 4.1 and 4.2), both loop–loop and loop–dislocation interaction energies have been calculated using MD simulations and have been compared with the results obtained from elasticity theory [13,47]. These calculations have led to the following main conclusions:

(a) The interaction between small loops at short distances cannot be described quantitatively by the isotropic elasticity and the infinitesimal loop approximation. The agreement improves for the long-range interactions between larger loops.
(b) The interaction between gliding clusters can lead to the formation of complexes of clusters which may act as a nucleation centre for a 'raft' of loops.
(c) In the case of Fe, the loop–dislocation interaction energy as a function of distance from an edge dislocation obtained by the atomistic simulations agrees quite well with results of the isotropic elasticity theory for distances down to ~1 nm from the edge dislocation. In the case of copper, however, the inter-

action between the dissociated edge dislocation and a SIA cluster is complicated since the strain field of the dislocation enhances the dissociation of the cluster and causes an increase in the dislocation–cluster interaction energy. In other words, the isotropic elasticity theory (without considering dissociation) would underestimate the interaction energy. At non-zero temperatures this difference can be even more pronounced due to differences in the mobility of pure edge (all clusters/loops in Fe) and dissociated (large clusters/loops in Cu) clusters.

These results imply that the results of analytical calculations and DD simulations regarding the stand-off distance and unlocking stress (Sections 4.1 and 4.2) are likely to be fairly realistic for bcc iron but somewhat less accurate for copper, the accuracy depending on the cluster/loop size (for details see [14]).

Finally, the details of interactions between a moving edge dislocation (under the action of an applied stress) and SFTs [48,49] in copper and voids [50] in bcc iron have been studied recently using MD. Results of these calculations are discussed in Ref. 14 and will not be repeated here. In general, the SFTs in copper are found to be strong obstacles to the dislocation glide and are likely to be destroyed by repeated interactions with dislocations eminating from the dislocation sources. In such interactions vacancies absorbed at the interacting dislocation segment may cause it to climb. Very recently, the interactions between the moving dislocation (under stress) and a row of voids have been investigated [50] over wide temperature and stress ranges. It is found that each time a dislocation interacts with a void, it absorbs a few vacancies and climbs. It was concluded that the repeated interactions may completely annihilate the voids.

These results validate at least qualitatively the assumptions made in the DD calculations of the lower yield stress and cleared channel formation described in Section 4.2. Details of the interaction energies between an edge dislocation and SFTs and voids and mechanisms of their interaction under different conditions (temperature, dislocation velocity, applied stress) will have to be carefully implemented in the DD calculations of the lower yield stress values.

5. Conclusions and perspectives

Experimental, theoretical and computer simulation results clearly demonstrate that the primary damage production in the cascades and properties of the clusters thus produced play a central role in damage accumulation and mechanical response of the irradiated materials. Clearly, these factors must be taken into account in realistic description of radiation hardening and plastic flow localization. While modelling various aspects of the material response, all known facts regarding the initial (pre-deformation) and post-deformation microstructures must be properly considered. Furthermore, it is vital that both the main assumptions and the main predictions of a particular model must be validated by experimental results or the results of other theoretical or computational calculations.

Results described and discussed in the present paper support the idea that the segregation of impurity atoms at and of clusters/loops in the vicinity of dislocations inhibits them from acting as dislocation sources. An overall increase in the threshold stress level for dislocation generation seems to be the main cause for the plastic flow localization and yield drop. Under these conditions, fresh dislocations are generated either at relatively weakly decorated dislocations or/and at points of stress/strain singularities (e.g. surfaces, interfaces, boundaries, etc.).

The phenomenon of yield drop provides a clear signature of the occurrence of plastic flow localization. The flow localization occurs in the form of cleared channels or deformation bands. The presence of strong and rigid obstacles to dislocation motion on the glide plane may prevent the formation and propagation of these bands.

Although some significant advances have been made in the understanding of irradiation hardening and plastic flow localization within the framework of the CISH model, a considerable amount of concerted effort (both experimental and theoretical) seems to be necessary to elucidate the following fundamental issues:

- sites and stress/strain level for the initiation of cleared channels,
- dynamics of dislocation–obstacle interactions in the cleared channels,
- mechanisms of defect removal (in the channels) and those controlling the width of the channels,
- kinetic effects of dislocation velocity on the consequences of dislocation–obstacle interactions,
- in cases where the plastic deformation occurs mainly in the cleared channels and the volumes between the channels remain practically undeformed, careful calculations are necessary to evaluate the global stress/strain response of a 'composite' material containing 'soft' cleared channel and 'hard' matrix.

Even though the calculated values of $\Delta\sigma^{l}$ taking only SFTs and voids as the main obstacles for gliding source dislocations in copper and iron, respectively, agree reasonably well with the experimental results, the contribution of the SIA loop population present in both copper and iron to $\Delta\sigma^{l}$ needs to be properly evaluated by combining the results of MD and 3-D dislocation dynamics simulations.

Acknowledgements

The present work was partly funded by the European Fusion Technology Programme and was supported by the US Department of Energy (DOE), Office of Fusion Energy Sciences (OFES) through grants DE-FG03-00ER54594 and DE-FG03-01ER54626 with UCLA. The authors would like to thank Dr Yu.N. Osetsky for helful comments and suggestions.

References

[1] E.P. Wigner, J. Appl. Phys. 17 (1946) 857.
[2] A.W. McReynolds, W. Augustiniak, M. McKewon, D.B. Rosenblatt, Phys. Rev. 98 (1955) 418.
[3] T.H. Blewitt, R.R. Coltman, R.E. Jamison, J. Redman, J. Nucl. Mater. 2 (1960) 277.
[4] M.J. Makin, in: W.F. Sheely (Ed.), Radiation Effects, AIME, vol. 37, 1966, p. 627, Metallurgical Soc. Conf., Asheville, N.C., September 1965, Gordon and Breach, Inc., New York.
[5] J. Diehl, in: A. Seeger, D. Schumacher, W. Schilling, J. Diehl, (Eds.), Vacancies and Interstitials in Metals, Proc. Int. Conf. KFA Jüich, 1968, North Holland Amsterdam, 1969, p. 739.
[6] B.N. Singh, A.J.E. Foreman, H. Trinkaus, J. Nucl. Mater. 249 (1997) 103.
[7] M. Victoria, N. Baluc, C. Bailat, Y. Dai, M.I. Luppo, R. Schäublin, B.N. Singh, J. Nucl. Mater. 276 (2000) 114.
[8] B.N. Singh, D.J. Edwards, P. Toft, J. Nucl. Mater. 299 (2001) 205.
[9] D.J. Edwards, B.N. Singh, J.B. Bilde-Sørensen, Philos. Mag. (A), submitted for publication.
[10] H. Trinkaus, B.N. Singh, A.J.E. Foreman, J. Nucl. Mater. 249 (1977) 91, 251 (1997) 171.
[11] Yu.N. Osetsky, D.J. Bacon, A. Serra, B.N. Singh, S.I. Golubov, J. Nucl. Mater. 276 (2000) 65.
[12] Yu.N. Osetsky, A. Serra, B.N. Singh, S.I. Golubov, Philos. Mag. A 80 (2000) 2131.
[13] Y.N. Osetsky, D.J. Bacon, A. Serra, B.N. Singh, MRS Symp. Proc. 653 (2001) Z3.4.
[14] Yu.N. Osetsky, D.J. Bacon, B.N. Singh, B.D. Wirth, these Proceedings.
[15] Yu.N. Osetsky, A. Serra, V. Priego, J. Nucl. Mater. 276 (2000) 202.
[16] D. Rodney, G. Martin, Phys. Rev. B 61 (2000) 8714.
[17] S.I. Golubov, X. Liu, H. Huang, C.H. Woo, Comp. Phys. Comm. 137 (2001) 312.
[18] N.M. Ghoniem, B.N. Singh, L.Z. Sun, T. Diaz de la Rubia, J. Nucl. Mater. 276 (2000) 166.
[19] H.M. Zbib, T. Diaz de la Rubia, M. Rhee, J.P. Hirth, J. Nucl. Mater. 276 (2000) 154.
[20] N.M. Ghoniem, S.-H. Tong, B.N. Singh, L.Z. Sun, Philos. Mag. A 81 (2001) 2743.
[21] N.M. Ghoniem, S.-H. Tong, J. Huang, B.N. Singh, M. Wen, these Proceedings.
[22] A.H. Cottrell, Theoretical Structural Metallurgy, Edward Arnold, London, 1955, p. 228.
[23] F.C. Frank, W.T. Read, Phys. Rev. 79 (1950) 722.
[24] C. Herring, J.K. Galt, Phys. Rev. 85 (1952) 1060.
[25] B.N. Singh, D.J. Edwards, P. Toft, J. Nucl. Mater. 238 (1996) 244.
[26] G. Saada, T. Washburn, J. Phys. Soc. Jpn. 18 (1963) 43.
[27] E. Orowan, Nature 149 (1942) 643.
[28] B.N. Singh, J. Comp. -Aided Mater. Des. 6 (1999) 195.
[29] B.N. Singh, H. Trinkaus, S.I. Golubov, in: K.H.J. Buschow, R.W. Cahn, M.C. Flemings, B. Ilschner, E.J. Kramer, S. Mahajan (Eds.), Encyclopedia of Materials: Science and Technology, vol. 8, Pergamon, Oxford, 2001, p. 7957.
[30] M. Eldrup, B.N. Singh, J. Nucl. Mater. 276 (2000) 269.
[31] M. Eldrup, B.N. Singh, S.J. Zinkle, T.S. Byun, K. Farrell, these Proceedings.
[32] J. Bently, B.L. Eyre, M.H. Loretto, US-ERDA Conf. 751006, Gatlinburg, 1975, p. 925.
[33] B.N. Singh, J.H. Evans, A. Horsewell, P. Toft, D.J. Edwards, J. Nucl. Mater. 223 (1995) 95.
[34] B.N. Singh, J.H. Evans, A. Horsewell, P. Toft, G.V. Müller, J. Nucl. Mater. 258–263 (1998) 865.
[35] B.N. Singh, A. Horsewell, P. Toft, J. Nucl. Mater. 271–272 (1998) 97.
[36] B.N. Singh, J.H. Evans, J. Nucl. Mater. 226 (1995) 277.
[37] B.N. Singh, A. Horsewell, P. Toft, in: J.P. Lynov, B.N. Singh (Eds.), Risø Report No. Risø-R-1070(EN) November, 1998, p. 41.
[38] D.J. Edwards, B.N. Singh, P. Toft, M. Eldrup, J. Nucl. Mater. 258–263 (1998) 978.
[39] B.N. Singh, D.J. Edwards, M. Eldrup, P. Toft, Risø Report No. Risø-R-1008 (EN), May 1998.
[40] B.N. Singh, M.R. Warren, P.D. Parson, in: C.T. John, B. Wyles, B. Moore (Eds.), Nuclear Fuel Performance, Proc. Int. Conf., London, 15–19 October 1973, British Nuclear Energy Soc. (BNES, 1973) p. 64.1.
[41] L.M. Howe, Radiat. Eff. 23 (1974) 181.
[42] B.N. Singh, J.F. Stubbins, P. Toft, Risø Report No. Risø-R-1128 (EN), March 2000.
[43] A. Seeger, in: Proceedings of Second UN International Conference On Peaceful Uses of Atomic Energy, Geneva, vol. 6, September 1958, p. 250.
[44] G.T. Hahn, Acta Metall. 10 (1962) 727.
[45] N.M. Ghoniem, B.N. Singh, in: J.B. Bilde-Sørensen, J.V. Carstensen, N. Hansen, D. Juul Jensen, T. Leffers, W. Pantleon, O.B. Pedersen, G. Winther (Eds.), Proceedings of the 20th Risø International Symposium on Materials and Sciences: Deformation-Induced Microstructures; Analysis and Relation to Properties, Risø National Laboratory, Roskilde, Denmark, 1999, p. 41.
[46] L.Z. Sun, N.M. Ghoniem, S.-H. Tong, B.N. Singh, J. Nucl. Mater. 283–287 (2000) 741.
[47] Yu.N. Osetsky, D.J. Bacon, F. Gao, A. Serra, B.N. Singh, J. Nucl. Mater. 283–287 (2000) 784.
[48] Yu.N. Osetsky, D.J. Bacon, 2000, unpublished work.
[49] T. Diaz de la Rubia, H. Zbib, J.A. Kraishi, B.D. Wirth, M. Victoria, M.J. Caturla, Nature 406 (2000) 871.
[50] Yu.N. Osetsky, D.J. Bacon, 2001, unpublished work.